5–14% (1, 3, 6) (1–3% of all recipients [1, 3, 4]). The mortality rate of all VZV infection is 9.7% (5); however, that of visceral VZV infection is unknown.

A number of clinical reports have appeared about visceral dissemination. Almost all reports show that visceral dissemination of VZV, so-called visceral zoster, leads to a fatal outcome. However, only a few studies so far have analyzed the clinical course and complications among a large number of patients with visceral zoster. Therefore, The Kanto Study Group for Cell Therapy (KSGCT) has conducted a retrospective study to elucidate the clinical features and treatment outcome of patients with visceral zoster who were treated at these institutions.

Patients and methods

The study included all patients who underwent allogeneic HSCT (allo-HSCT) at hospitals belonging to the KSGCT between January 1994 and June 2005. Among 3129 patients, the 718 patients who died within 100 days of HSCT were not included in this analysis. The clinical features of 2411 patients were reviewed in detail. All patients were given prophylaxis with acyclovir (ACV) against herpes simplex virus beginning 7 ± 3 days before transplantation. The dose, duration, and mode of ACV prophylaxis varied.

Visceral dissemination (visceral VZV infection) was defined as histological or cultural evidence of internal organ involvement or clinical evidence of internal organ involvement without other identifiable causes.

Results

Incidence and characteristics of patients with visceral VZV infection after HSCT

Visceral VZV infection occurred in 20 (0.8%) of the 2411 patients. Among those 20 patients, 6 patients had a positive blood test. Two autopsies and 1 necropsy were performed. The clinical characteristics of the patients developing visceral VZV infection are shown in Table 1. The median age was 36 years (range 23–63), and 12 patients (60%) were male. The majority received myeloablative transplants for hematological malignancy. Twelve (70%) of 17 patients who could be examined were seropositive for VZV before transplantation. Only 1 of 5 patients, who were seronegative for VZV before transplantation, was thought to be primarily infected with VZV. Fourteen patients developed Grade 0–I acute graft-versus-host disease (GVHD), and Grade II–IV acute GVHD was observed in 6 patients. Sixteen patients (80%) had chronic GVHD and 17 patients (85%) were receiving immunosuppressive therapy at the onset of visceral VZV infection. Seventeen patients who developed visceral VZV infection were not administered prophylactic ACV at the time of onset.

Characteristics of patient with visceral varicella zoster virus (VZV) infection

Age in years	
Median (range)	36 (23–63)
Gender	
Male	12
Female	8
Donor	
Related	7
Unrelated	13
Conditioning regimen	
Myeloablative	16
Nonmyeloablative	4
Prior SCT	
None	15
Once	5
GVHD prophylaxis	
FK506 + sMTX	8
FK506	2
CsA + sMTX	8
CsA	2
Acute GVHD	
Grade 0–1	14
Grade 2–4	6
Chronic GVHD	
Yes	17
No	3
VZV serostatus before SCT	
Positive	12
Negative	5
Unknown	3
Acyclovir prophylaxis	
Start of prophylaxis	Day −7 (−8 ~ −5)
End of prophylaxis	Day 35 (14–207)
Dose of prophylaxis	1000 mg (200–1000)

SCT, stem cell transplantation; GVHD, graft-versus-host disease; FK506, tacrolimus; CsA, cyclosporine; sMTX, short-term methotrexate.

Table 1

Clinical course of visceral VZV infection

The clinical data for patients with visceral VZV infection are summarized in Table 2. Twenty patients developed visceral VZV infection at a median of 273 (range 103–800) days after HSCT. Six patients (30%) had onset of infection after 1 year from the time of transplantation. The first symptom of visceral VZV infection was abdominal pain in 16 patients (80%), unconsciousness in 3 patients (15%), and no symptoms in 1 patient (5%). The abdominal pain was an acute and severe epigastric pain. Eighteen patients (90%) had vesicular eruptions. Vesicular eruptions appeared in most patients (11/18 patients, 61%) from 2 to 4 days after onset of abdominal pain or unconsciousness. Only 2 patients had vesicular eruptions on the same day that they experienced abdominal pain or unconsciousness. Vesicular eruptions were disseminated in 16 patients (89%), and were localized as a single lesion in 2 patients (11%). Among 18 patients with vesicular eruptions, all 7 patients who received the test were seropositive for VZV antigen from skin vesicular fluid. Seven patients among 11 who did not receive the test for VZV antigen were seropositive by the polymerase chain reaction (PCR) test from either blood or cerebrospinal fluid specimens.

Two patients without any eruptions were diagnosed as having a visceral VZV infection; 1 patient was diagnosed at autopsy and the other patient was diagnosed by the VZV PCR test for blood and cerebrospinal fluid. The former patient was treated with only steroids for chronic GVHD and bronchiolitis obliterans at the time of VZV infection. He had no signs of eruptions or abdominal pain and died from progressive respiratory failure and fulminant hepatitis. The latter patient was also treated with tacrolimus and steroids for chronic GVHD when he lost consciousness as the first symptom of visceral VZV infection.

Clinical course of visceral varicella zoster virus (VZV) infection

First sign of visceral VZV infection	
Abdominal pain	16
Unconsciousness	3
No sign	1
Vesicular eruptions	
Yes	18
No	2
Presentation of vesicular eruptions	
Dermatomal dissemination	16
Dermatomal localization	2
Median onset of infection (range)	Day 273 (103–800)
Median day of eruptions (range)	Day 276 (114–803)
Median day of eruptions after onset (range)	3 days (0–13)
Survived	16
Died	4

Table 2

Treatment and outcome

Nineteen patients were treated with intravenous (IV) ACV. ACV was initially administered at a dosage of 1500 mg/day to 12 patients; 6 patients were treated with <1500 mg/day. One patient received ACV and foscarnet therapy. The median length of treatment was 13 (range 1–40) days. Four patients died within 5 days after the start of treatment.

Three of the 18 patients who had vesicular eruptions were treated with IV ACV before the appearance of eruptions, and all 3 patients survived (Fig. 1). Twelve patients received IV ACV on the same day of the appearance of eruptions and 1 of those patients died. Three patients were given IV ACV after the appearance of eruptions and 2 of those patients died.

The mortality of visceral VZV infection was 20% (4 of 20 patients). Three of the 4 patients had abdominal pain and vesicular eruptions. However, 1 patient did not have abdominal pain or vesicular eruptions. All 4 patients developed fulminant hepatitis and multiple organ failure within 9 days of the onset of infection. Two autopsies and 1 necropsy revealed intranuclear inclusion bodies in the liver. VZV was positive in the inclusion bodies based on immunohistological staining in these 3 cases.

Discussion

Twenty of 2411 recipients of allo-HSCT (0.8%) developed a visceral VZV infection. The incidence of this study is consistent with previous reports (about 1%) (1, 3, 4).

Patients presented with visceral VZV infection at a mean of 273 days after transplantation. Previous reports have shown that most serious VZV infections including visceral zoster develop at between 1 and 9 months (3–5). The mean time of onset in the current series was later than in previous reports. Seventeen patients among 20 patients had chronic GVHD at the presentation with visceral VZV. Nine patients among the 17 had the onset of the infection after 9 months, while 8 patients developed visceral VZV infection before 9 months. The present results suggest that all

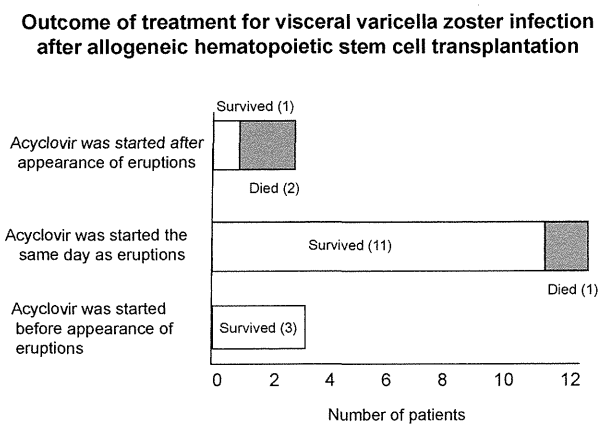

Fig. 1. Outcome of treatment for visceral varicella zoster virus infection after allogeneic hematopoietic stem cell transplant. Treatment with intravenous acyclovir was started before the appearance of eruptions in 3 of the 18 patients who had vesicular eruptions (all 3 survived); the same day in 12 patients (11 survived, 1 died); and after the appearance of eruptions in 3 patients (1 survived, 2 died).

patients with active GVHD had visceral VZV infection even later than 9 months after transplantation.

Most clinical symptoms of visceral VZV infection are associated with abdominal pain in many case reports. David et al. (4) reported that all 10 patients had abdominal pain at the onset. The symptoms of visceral VZV infection in the current series were abdominal pain (80%), unconsciousness (15%), and no symptoms (5%). The pain was located in the epigastric region and dissimilar from the dermatome-limited pain that can characterize the zoster prodrome. This pain was most likely a result of stretching of the Glisson's capsule secondary to hepatitis, VZV-induced pancreatitis, or VZV gastritis (4).

Eighteen patients (90%) had vesicular eruptions, and 2 (10%) had no eruptions. Although many patients present with eruptions, some reports (6–9) reveal patients without eruptions of VZV infection. The occurrence of visceral dissemination in HSCT recipients without any signs of cutaneous disease demonstrates that cell-associated viremia can occur without replication of the virus in skin, presumably by entry of virus into T cells that traffic through sensory ganglia (5, 6).

The current study demonstrates that the mortality rate of visceral VZV infection in recipients of allo-HSCT is 20%. Previous studies (4, 5) showed that the mortality is about 50% among patients with visceral dissemination. David et al. (4) reported that the mean time interval from onset of visceral symptoms to diagnosis was 7 days (range 4–14 days). Antiviral therapy was promptly initiated after the diagnosis of varicella infection. On the other hand, 15 (83%) of the 18 patients with vesicular eruptions in the current study were treated with IV ACV before or on the same day that the eruptions appeared. The interval from onset to diagnosis was shorter than that previously reported (4).

Several studies have shown that long-term prophylactic ACV at 400 mg/day, which is continued until the end of immunosuppressive therapy, successfully decreases the cumulative incidence of VZV disease, even after the discontinuation of ACV (10–12). However, 3 of the patients who developed visceral VZV infection in the current series were on prophylactic ACV at the time of onset. All of these patients were treated with immunosuppressive agents, and the onset of infection was on day 118, day 175, and day 210. Two patients were given 200 mg/day of ACV and 1 patient received 600 mg/day. We did not examine susceptibility to the virus. However, as all 3 patients could respond to the treatment, we assumed that they did not have the resistant virus. These results suggest that patients who are on prophylactic ACV may develop visceral zoster.

Administration of empiric therapy before the appearance of eruptions contributed to patient survival (Fig. 1). Therefore, early IV treatment using an appropriate dosage is effective. Hence, early diagnosis and treatment are important.

In summary, visceral VZV infection after allo-HSCT is a rare complication, but it is associated with high mortality. The possibility of a visceral VZV infection must be considered when patients with chronic GVHD or those being treated with immunosuppressive agents demonstrate abdominal pain or unconsciousness. Therefore, such patients should receive early IV treatment using 30 mg/kg of ACV/day. In conclusion, patients who are on prophylactic ACV are still at risk of developing visceral VZV infection.

Acknowledgements:

Thanks: The authors thank Dr. N. Oyaizu (Department of Laboratory Medicine, Institute of Medical Science, University of Tokyo) for immunohistochemistry analyses.

Conflict of interest: The authors declare no conflict of interest.

References

1. Koc Y, Miller KB, Schenkein DP, et al. Varicella zoster virus infections following allogeneic bone marrow transplantation: frequency, risk factors, and clinical outcome. Biol Blood Marrow Transplant 2000; 6: 44–49.

2. Steer CB, Szer J, Sasadeusz J, Matthews JP, Beresford JA, Grigg A. Varicella-zoster infection after allogeneic bone marrow transplantation: incidence, risk factors and prevention with low-dose acyclovir and ganciclovir. Bone Marrow Transplant 2000; 25: 657–664.
3. Han CS, Miller W, Haake R, Weisdorf D. Varicella zoster infection after bone marrow transplantation: incidence, risk factors and complications. Bone Marrow Transplantation 1994; 13: 277–283.
4. David DS, Tegtmeier BR, O'Donnell MR, Paz IB, McCarty TM Visceral varicella-zoster after bone marrow transplantation: report of a case series and review of the literature. Am J Gastroenterol 1998; 93: 810–813.
5. Locksley RM, Flournoy N, Sullivan KM, Meyers JD. Infection with varicella-zoster virus after bone marrow transplantation. J Infect Dis 1985; 152: 1172–1181.
6. Arvin AM. Varicella-zoster virus: pathogenesis, immunity, and clinical management in hematopoietic cell transplant recipients. Biol Blood Marrow Transplant 2000; 6: 219–230.
7. Meylan PR, Miklossy J, Iten A, et al. Myelitis due to varicella-zoster virus in an immunocompromised patient without a cutaneous rash. Clin Infect Dis 1995; 20: 206–208.
8. Rogers SY, Irving W, Harris A, Russell NH. Visceral varicella zoster infection after bone marrow transplantation without skin involvement and the use of PCR for diagnosis. Bone Marrow Transplant 1995; 15: 805–807.
9. Yagi T, Karasuno T, Hasegawa T, et al. Acute abdomen without cutaneous signs of varicella zoster virus infection as a late complication of allogeneic bone marrow transplantation: importance of empiric therapy with acyclovir. Bone Marrow Transplant 2000; 25: 1003–1005.
10. Thomson KJ, Hart DP, Banerjee L, Ward KN, Peggs KS, Mackinnon S. The effect of low-dose acyclovir on reactivation of varicella zoster virus after allogeneic haemopoietic stem cell transplantation. Bone Marrow Transplant 2005; 35: 1065–1069.
11. Kanda Y, Mineishi S, Saito T, et al. Long-term low-dose acyclovir against varicella-zoster virus reactivation after allogeneic hematopoietic stem cell transplantation. Bone Marrow Transplant 2001; 28: 689–692.
12. Erard V, Guthrie KA, Varley C, et al. One year acyclovir prophylaxis for preventing varicella-zoster virus disease after hematopoietic cell transplantation: no evidence of rebound varicella-zoster virus disease after drug discontinuation. Blood 2007; 110: 3071–3077.

Available online at www.sciencedirect.com

SciVerse ScienceDirect

American Journal of OTOLARYNGOLOGY

ELSEVIER

American Journal of Otolaryngology–Head and Neck Medicine and Surgery 34 (2013) 89–92

www.elsevier.com/locate/amjoto

Progressive hearing loss following acquired cytomegalovirus infection in an immunocompromised child

Ken Kato, MD[a,*], Hironao Otake, MD, PhD[a], Mitsuhiko Tagaya, MD, PhD[a], Yoshiyuki Takahashi, MD, PhD[b], Yoshinori Ito, MD, PhD[b], Asahito Hama, MD, PhD[b], Hideki Muramatsu, MD, PhD[b], Seiji Kojima, MD, PhD[b], Shinji Naganawa, MD, PhD[c], Tsutomu Nakashima, MD, PhD[a]

[a]*Department of Otorhinolaryngology, Nagoya University Graduate School of Medicine, 65, Tsurumai-cho, Showa-ku, Nagoya, Japan*
[b]*Department of Pediatrics, Nagoya University Graduate School of Medicine, Nagoya, Japan*
[c]*Department of Radiology, Nagoya University Graduate School of Medicine, Nagoya, Japan*

Received 23 August 2012

Abstract We report a rare case of progressive hearing loss after acquired CMV infection in a child with Langerhans cell histiocytosis (LCH). A 5-month-old female was diagnosed as having LCH. When she was 14 months old, she received an unrelated donor umbilical cord blood transfusion for the treatment of intractable LCH. CMV infection was confirmed after the blood transfusion. Because her own umbilical cord had no CMV, the CMV infection was not congenital. When she was 7 years old, mixed hearing loss was noted with bilateral otitis media with effusion. After that time, the sensorineural hearing loss progressed to bilateral profound hearing loss over 3 years. Three-dimensional fluid-attenuated inversion recovery magnetic resonance imaging with gadolinium contrast enhancement revealed a high intensity area in the inner ear that suggested bilateral labyrinthitis. This case demonstrates the possibility that, under the immunodeficiency, the acquired CMV infection causes progressive sensorineural hearing loss.

1. Introduction

Cytomegalovirus (CMV) is a DNA-containing herpes virus. Its scientific name is human herpes virus 5 and it causes a range of symptoms after the first infection or after reactivation. CMV is well known as the cause of congenital sensorineural hearing loss or the opportunistic pathogen. Congenital CMV infection, which is caused by transplacental infection, also has various symptoms including low birth weight, microcephaly, hepatosplenomegaly, meningitis, and sensorineural hearing loss. Congenital CMV infection is the most widespread cause of sensorineural hearing loss other than inherited disease [1–6]. However, few reports have described sensorineural hearing loss caused by acquired CMV infection. We report progressive sensorineural hearing loss caused by acquired CMV infection in an immunocompromised child.

2. Case report

A 5-month-old female was referred to the Department of Pediatrics at Nagoya University Hospital because of fever, lymphadenopathy and purpura. Based on histological examination of neck lymph nodes, she was diagnosed with disseminate Langerhans cell histiocytosis (LCH). Then she received chemotherapy. First, one course of DAL-HX 83 study group protocol (etoposide (VP-16)+vinblastine (VBL)+prednisolone (PDN)) as initial chemotherapy and secondly, one course of next chemotherapy (VP-16+VBL+cyclophosphamide (CPA)) were performed. But the LCH did not response completely. When she was 9 months old, her splenomegaly became worse and caused C-reactive protein

* Corresponding author. Department of Otorhinolaryngology, Nagoya University Graduate School of Medicine, 65, Tsurumai-cho, Showa-ku, Nagoya 466-8550, Japan. Tel.: +82 52 744 2323; fax: +82 52 744 2325.
E-mail address: katoken@med.nagoya-u.ac.jp (K. Kato).

0196-0709/$ – see front matter © 2013 Elsevier Inc. All rights reserved.
http://dx.doi.org/10.1016/j.amjoto.2012.09.006

(CRP) elevation and anemia had progressed. Although she was given blood transfusions many times, her anemia did not improve. Finally, splenectomy was performed. After the operation, two courses of CHOP therapy (CPA+VP-16+vincristine (VCR)+PDN) and then, one course of next chemotherapy (CPA+VP-16+VCR) were performed but her symptom such as fever elevation, anemia, thrombocytopenia, and liver dysfunction became worse.

When she was 14 months old, finally, a cord stem cell transplant from an unrelated donor was performed and her LCH improved. However, CMV infection that was recognized before the cord stem cell transplantation was continuing. Because CMV antigen was not detected in her own cord blood, it was considered that the CMV infection was not congenital infection but acquired during treatment of the LCH. Due to her immunodeficiency with few CD4+ T cells (< 100/μl–400/μl), CMV infection continued including retinitis. CMV retinitis started when she was 18 months old. She was administered the antiviral drugs ganciclovir and foscarnet. During treatment, CMV antigen became negative, but when the antiviral drugs were discontinued, it became positive again, and she underwent repeated hospitalization and discharge. The retinitis did not become worse during this period. Fig. 1 shows changes of CMV-DNA amount that was investigated from the age of seven. When she was 7 years old, CMV DNA increased to 3913 copies/ml, and then decreased to zero or hundreds of copies/ml. When she was 9 years old, CMV DNA increased to 8705 copies/ml, but again decreased to zero or hundreds of copies/ml. Together with antiviral drug therapy, she was transfused with activated CD4+ T cells. Her blood CD4+ T cells increased to within the range of 500–900/μl, but her immunodeficiency did not improve. Her CMV antigen periodically became positive, at which times it was necessary to administer foscarnet.

When she was 6 years old, she consulted the Department of Otorhinolaryngology in our hospital because of suspicion of otitis media. At that time her mother did not notice her hearing impairment. However, three months after her first visit to the Department of Otorhinolaryngology, mixed hearing impairment with otitis media (OME) with effusion was recognized bilaterally (first audiogram in Fig. 2). A half year later, bilateral tympanostomy and ventilation tube insertion were performed because OME did not improve. Her bone-conduction hearing levels deteriorated to profound hearing loss (Fig. 2). When she was 8 years old, she complained of dizziness transiently. Three-dimensional fluid-attenuated inversion recovery (3D-FLAIR) MRI before and after enhancement showed a high intensity lesion in the internal auditory canal and in the cochlea without inner ear malformation. When she was 11 years old, 3D-FLAIR MRI after enhancement was performed again. The signal intensity of internal auditory canal was much stronger than that taken when she was 8 years old (Fig. 3). These findings suggested the exacerbation of meningitis close to the inner ear. When she was 11 years old, she had inflammation of the ventricles of the brain and a large amount of CMV-DNA was detected from her cerebrospinal fluid.

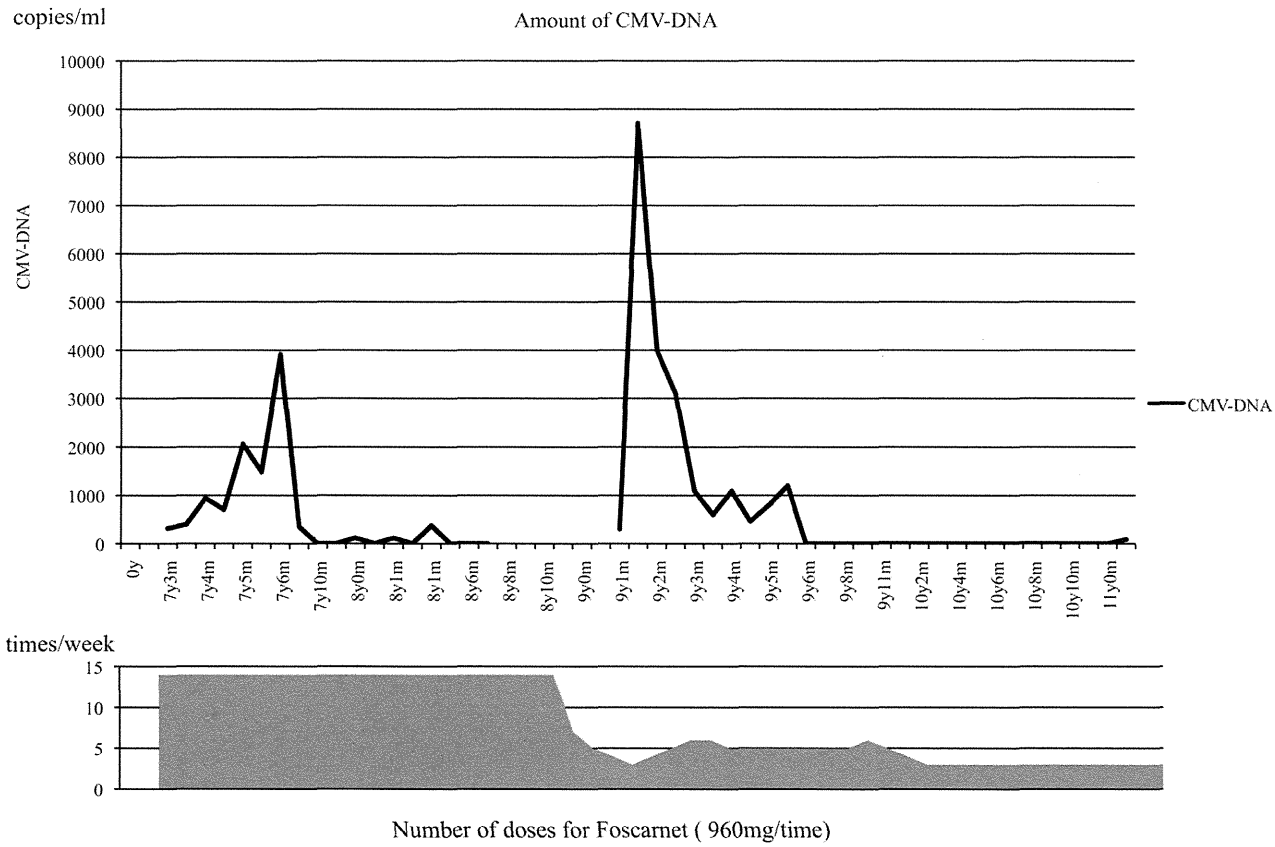

Fig. 1. The upper panel shows the changes in CMV DNA numbers from when she was 7 years old through when she was 11 years old. The lower panel shows the frequency of foscarnet administration during this period.

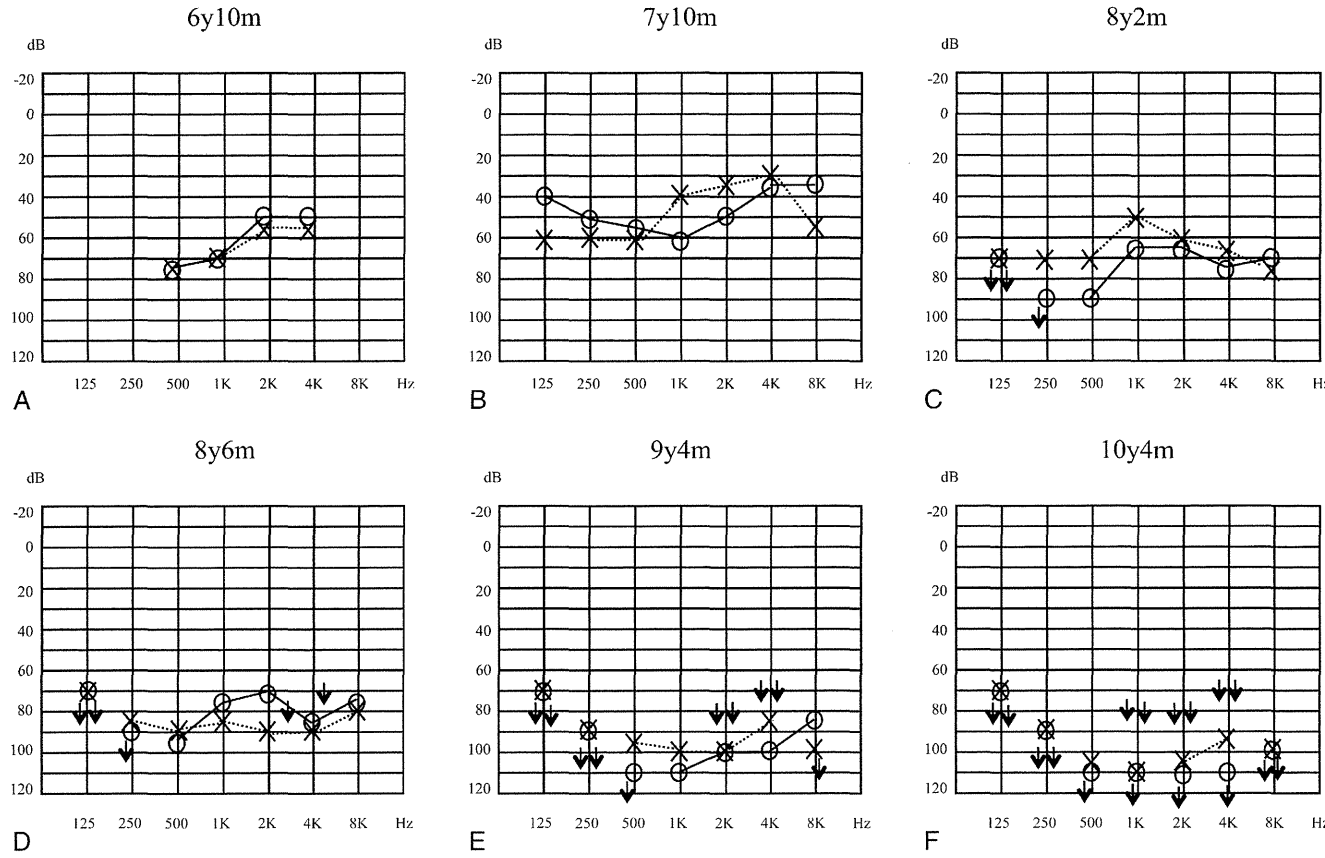

Fig. 2. From January 2007 to the present, the patient's hearing level has deteriorated. In particular, her bony conductive hearing level became worse. This showed that her sensorineural hearing loss was progressing.

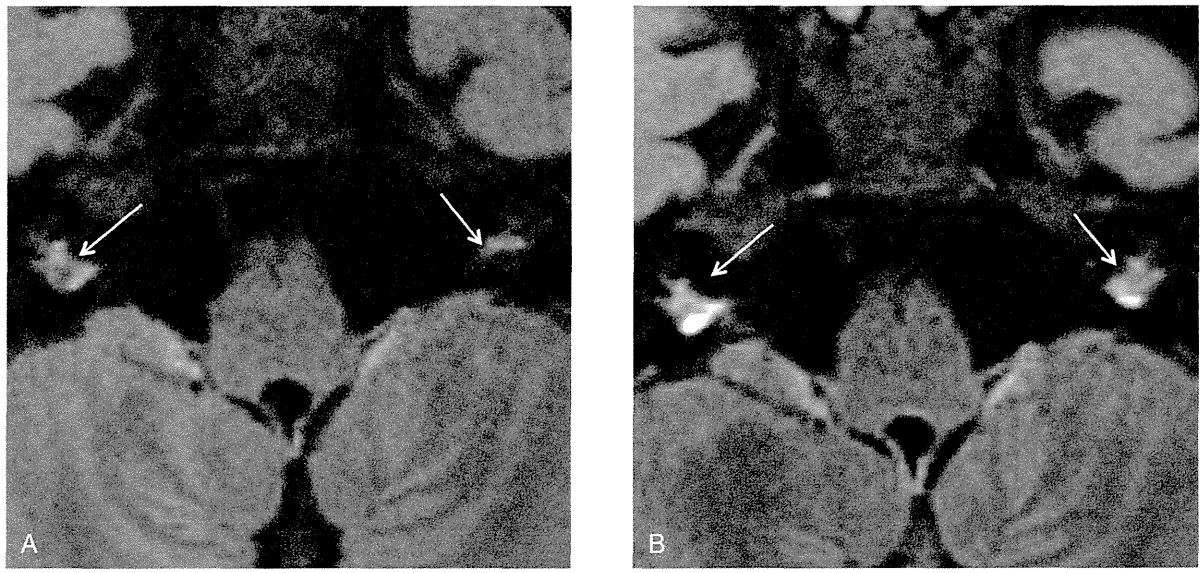

Fig. 3. 3D-FLAIR MRI after intervenous gadolinium administration. A was taken when she was 8 years old, and B was when she was 11 years old. The gadolinium enhancement of the internal auditory canal indicated by arrows was stronger in B than in A.

3. Comments

Because congenital CMV infection is transplacental infection, CMV is detected from the dried umbilical cord. On the contrary, in acquired CMV infection, CMV is not detected from the umbilical cord [7,8]. We diagnosed this case as acquired CMV infection since CMV was not detected from dried umbilical cord blood, we diagnosed that it was acquired CMV infection. There were few papers that described progressive sensorineural hearing loss in patients with acquired CMV infection except for the two cases reported by Meynard et al. [9]. These patients were also infected with human immunodeficiency virus (HIV) and were immunodeficient. Our patient is also suffering from immunodeficiency because of her allogeneic cord stem cell transplantation. Thus, her condition is similar to these cases where it was presumed that sensorineural hearing loss was caused by opportunistic infection.

In animal studies, CMV-infected cells have been detected in the perilymph area and spinal ganglion, but not in the endolymph area or hair cells [4,10,11]. Katano et al. [4] and Schraff et al. [11] injected CMV into the inner ear of guinea pigs and observed severe inflammation and bleeding in the scala tympani and spiral ganglion with progressive hearing loss. Virally encoded macrophage inflammatory proteins play the important role of inflammation in the scala tympani and CMV-related hearing loss [11]. Sugiura et al. [12] and Nardo et al. [13] succeeded in detecting CMV DNA in the inner ear fluid of congenitally or acquired CMV-infected patients who received cochlear implants. In these patients, CMV DNA was not detected in peripheral blood mononuclear cell. These articles are indirect evidence of CMV affinity and activity in the inner ear. In the temporal bone of patients congenitally infected with CMV, many pathologic findings such as endolabyrinthitis, endolymphatic hydrops, loss of cochlear hair cells and CMV infecting many parts of the cochlea and the vestibular system are observed [5,6]. Bachor et al. [14] reported their findings in the temporal bone of patients with acquired CMV infection. In our patient, the existence of asymptomatic meningitis and labyrinthitis was recognized by 3D-FLAIR MRI.

4. Conclusion

We experienced a case with progressive sensorineural hearing loss following acquired CMV infection in an immunocompromised child with Langerhans cell histiocytosis (LCH). To detect labyrinthitis, 3D-FLAIR MRI was very useful.

References

[1] Catherine S, Peckam SE. Cytomegalovirus in the neonate. J Antimicrob Chemother 1989;23:17-21.
[2] Noorbakhsh S, Siadati A, Farhadi M, et al. Role of cytomegalovirus in sensorineural hearing loss of children: a case–control study Teheran, Iran. Int J Pediatr Otorhinolaryngol 2008;72:203-8.
[3] Usami S. Hearing loss and virus infection. MB ENT 2009;99:8-16.
[4] Katano H, Sato Y, Tsutsumi Y, et al. Pathogenesis of cytomegalovirus-associated labyrinthitis in guinea pig model. Microbes Infect 2007;9:183-91.
[5] Rarey KE, Davis LD. Temporal bone histopathology 14 years after cytomegalic inclusion disease: a case study. Laryngoscope 1993;103: 904-9.
[6] Strauss M. Human cytomegalovirus labyrinthitis. Am J Otolaryngol 1990;11:292-8.
[7] Ikeda S, Tsuru A, Moriuchi M, et al. Retrospective diagnosis of congenital cytomegalovirus infection using umbilical cord. Pediatr Neurol 2006;34:415-6.
[8] Mizuno T, Sugiura S, Kimura H, et al. Detection of cytomegalovirus DNA in preserved umbilical cords from patients with sensorineural hearing loss. Eur Arch Otorhinolaryngol 2009;266:351-5.
[9] Meynard JL, Amrani ME, Meyohas MC, et al. Two cases of cytomegalovirus infection revealed by hearing loss in HIV-infected patients. Biomed Phamacother 1997;51:461-3.
[10] Harris JP, Fan JT, Keithley EM. Immunologic responses in experimental cytomegalovirus labyrinthitis. Am J Otolaryogol 1990;11:304-8.
[11] Schraff SA, Schleiss MR, Brown DK, et al. Macrophage inflammatory proteins in cytomegalovirus-related inner ear injury. Otolaryngol Head Neck Surg 2007;137:612-8.
[12] Sugiura S, Yoshikawa T, Nishiyama Y, et al. Detection of human cytomegalovirus DNA in perilymph of patients with sensorineural hearing loss using real-time PCR. J Med Virol 2003;69:72-5.
[13] Nardo WD, Cattani P, Scorpecci A, et al. Cytomegalovirus DNA retrieval in the inner ear fluids of a congenitally deaf child one month after primary infection: a case report. Laryngoscope 2011;121:828-30.
[14] Bachor E, Suduhoff H, Litscel R, et al. The pathology of the temporal bones of child with acquired cytomegalovirus infection: studies by light microscopy, immunohistochemistry and polymerase-chain reaction. Int J Pediatr Otorhinolaryngol 2000;55:215-24.

blood

2013 121: 862-863
doi:10.1182/blood-2012-11-465633

Rabbit antithymocyte globulin and cyclosporine as first-line therapy for children with acquired aplastic anemia

Yoshiyuki Takahashi, Hideki Muramatsu, Naoki Sakata, Nobuyuki Hyakuna, Kazuko Hamamoto, Ryoji Kobayashi, Etsuro Ito, Hiroshi Yagasaki, Akira Ohara, Akira Kikuchi, Akira Morimoto, Hiromasa Yabe, Kazuko Kudo, Ken-ichiro Watanabe, Shouichi Ohga and Seiji Kojima

Blood (print ISSN 0006-4971, online ISSN 1528-0020), is published weekly by the American Society of Hematology, 2021 L St, NW, Suite 900, Washington DC 20036.

To the editor:

Rabbit antithymocyte globulin and cyclosporine as first-line therapy for children with acquired aplastic anemia

Horse antithymocyte globulin (hATG) and cyclosporine have been used as standard therapy for children with acquired aplastic anemia (AA) for whom an HLA-matched family donor is unavailable. However, in 2009, hATG (lymphoglobulin; Genzyme) was withdrawn and replaced by rabbit ATG (rATG; thymoglobulin; Genzyme) in Japan. Many other countries in Europe and Asia are facing the same situation.[1] Marsh et al recently reported outcomes for 35 adult patients with AA who were treated with rATG and cyclosporine as a first-line therapy.[2] Although the hematologic response rate was 40% at 6 months, several patients subsequently achieved late responses. The best response rate was 60% compared with 67% in a matched-pair control group of 105 patients treated with hATG. The overall and transplantation-free survival rates appeared to be significantly inferior with rATG compared with hATG at 68% versus 86% ($P = .009$) and 52% versus 76% ($P = .002$), respectively. These results are comparable to those from a prospective randomized study reported by Scheinberg et al comparing hATG and rATG.[3] Both studies showed the superiority of hATG over rATG.[2,3]

We recently analyzed outcomes for 40 Japanese children (median age, 9 years; range, 1-15) with AA treated using rATG and cyclosporine. The median interval from diagnosis to treatment was 22 days (range, 1-203). The numbers of patients with very severe, severe, and nonsevere disease were 14, 10, and 16, respectively. The ATG dose was 3.5 mg/kg/day for 5 days. The median follow-up time for all patients was 22 months (range, 6-38). At 3 months, no patients had achieved a complete response (CR) and partial response (PR) was seen in only 8 patients (20.0%). At 6 months, the numbers of patients with CR and PR were 2 (5.0%) and 17 (42.5%), respectively. After 6 months, 5 patients with PR at 6 months had achieved CR and 4 patients with no response at 6 months had achieved PR, offering a total best response rate of 57.5%. Two patients relapsed at 16 and 19 months without receiving any second-line treatments. Two patients with no response received a second course of rATG at 13 and 17 months, but neither responded. Sixteen patients underwent hematopoietic stem cell transplantation (HSCT) from alternative donors (HLA-matched unrelated donors, n = 13; HLA-mismatched family donors, n = 3). Two deaths occurred after rATG therapy, but no patients died after HSCT. Causes of death were intracranial hemorrhage at 6 months and acute respiratory distress syndrome at 17 months. The overall 2-year survival rate was 93.8% and the 2-year transplantation-free survival rate was 50.3% (Figure 1).

In our previous prospective studies with hATG, the response rates after 6 months were 68% and 70%, respectively, with no increases in response rates observed after 6 months.[4,5] Our results support the notion that rATG is inferior to hATG for the treatment of AA in children. First-line HSCT from an alternative donor may be justified, considering the excellent outcomes in children who received salvage therapies using alternative donor HSCT.

Yoshiyuki Takahashi
Department of Pediatrics, Nagoya Graduate School of Medicine, Nagoya, Japan

Hideki Muramatsu
Department of Pediatrics, Nagoya Graduate School of Medicine, Nagoya, Japan

Naoki Sakata
Department of Pediatrics, Kinki University School of Medicine, Osaka, Japan

Nobuyuki Hyakuna
Center of Bone Marrow Transplantation, Ryukyu University Hospital, Okinawa, Japan

Kazuko Hamamoto
Department of Pediatrics, Hiroshima Red Cross Hospital, Hiroshima, Japan

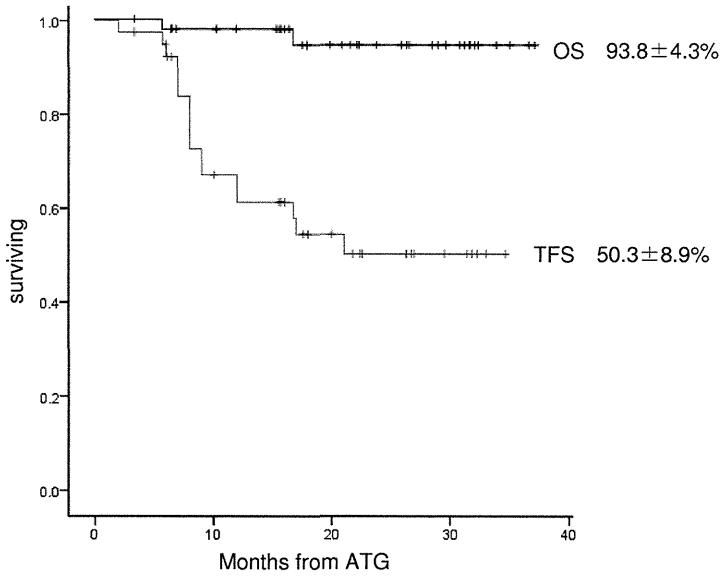

Figure 1. Kaplan-Meier estimates of overall survival (OS) and transplantation-free survival (TFS) in 40 Japanese children with AA. Survival was investigated using Kaplan-Meier methods. OS for all patients with AA after rATG and cyclosporine as first-line therapy included patients who later received HSCT for nonresponse to rATG. In the analysis of TFS for all patients treated with rATG and CSA, transplantation was considered an event.

Ryoji Kobayashi
Department of Pediatrics, Sapporo Hokuyu Hospital, Sapporo, Japan

Etsuro Ito
Department of Pediatrics, Hirosaki University School of Medicine, Hirosaki, Japan

Hiroshi Yagasaki
Department of Pediatrics, School of Medicine, Nihon University, Tokyo, Japan

Akira Ohara
Division of Blood Transfusion, Toho University Omori Hospital, Tokyo, Japan

Akira Kikuchi
Department of Pediatrics, Teikyo University School of Medicine, Tokyo, Japan

Akira Morimoto
Department of Pediatrics, Jichi Medical University School of Medicine, Tochigi, Japan

Hiromasa Yabe
Department of Cell Transplantation and Regenerative Medicine, Tokai University School of Medicine, Isehara, Japan

Kazuko Kudo
Division of Hematology and Oncology, Shizuoka Children's Hospital, Shizuoka, Japan

Ken-ichiro Watanabe
Department of Pediatrics, Graduate School of Medicine, Kyoto University, Kyoto, Japan

Shouichi Ohga
Department of Perinatal and Pediatric Medicine, Graduate School of Medical Sciences, Kyushu University, Fukuoka, Japan

Seiji Kojima
Department of Pediatrics, Nagoya Graduate School of Medicine, Nagoya, Japan

on behalf of the Japan Childhood Aplastic Anemia Study Group

Conflict-of-interest disclosure: The authors declare no competing financial interests.

Correspondence: Dr Seiji Kojima, Nagoya Graduate School of Medicine, Tsurumai-cho 65, Showa-ku, Nagoya, Ai, Japan 466-8550; e-mail: kojimas@med.nagoya-u.ac.jp.

References

1. Dufour C, Bacigalupo A, Oneto R, et al. Rabbit ATG for aplastic anaemia treatment: a backward step? *Lancet.* 2011;378(9806):1831-1833.
2. Marsh JC, Bacigalupo A, Schrezenmeier H, et al. Prospective study of rabbit antithymocyte globulin and cyclosporine for aplastic anemia from the EBMT Severe Aplastic Anaemia Working Party. *Blood.* 2012;119(23):5391-5396.
3. Scheinberg P, Nunez O, Weinstein B, et al. Horse versus rabbit antithymocyte globulin in acquired aplastic anemia. *N Engl J Med.* 2011;365(5):430-438.
4. Kojima S, Hibi S, Kosaka Y, et al. Immunosuppressive therapy using antithymocyte globulin, cyclosporine, and danazol with or without human granulocyte colony-stimulating factor in children with acquired aplastic anemia. *Blood.* 2000;96(6):2049-2054.
5. Kosaka Y, Yagasaki H, Sano K, et al. Prospective multicenter trial comparing repeated immunosuppressive therapy with stem-cell transplantation from an alternative donor as second-line treatment for children with severe and very severe aplastic anemia. *Blood.* 2008;111(3):1054-1059.

To the editor:

Peripheral blood stem cells versus bone marrow in pediatric unrelated donor stem cell transplantation

The relative benefits and risks of peripheral blood stem cells (PBSCs) versus bone marrow (BM) for allogeneic hematopoietic stem cell transplantation (SCT) are still a matter of highly controversial debates.[1-3] The first randomized study comparing the 2 stem cell sources in unrelated donor SCT recently documented comparable overall and event-free survival, but indicated a higher risk for chronic graft-versus-host disease (GVHD) with PBSCs.[4] Only a few pediatric patients were included in this study even though the long-term sequelae of chronic GVHD are of particular concern in this patient group.

We retrospectively compared the long-term outcome of contemporaneous unrelated donor SCT in 220 children transplanted with BM (n = 102) or PBSCs (n = 118) for hematologic malignancies and reported to the German/Austrian pediatric registry for SCT. All patients had received myeloablative conditioning followed by unmanipulated SCT from HLA-matched unrelated donors. The PBSC and BM groups were comparable with regard to patient and donor age, sex, cytomegalovirus (CMV) serostatus, disease status at transplantation, GVHD prophylaxis, growth factor use, and degree of HLA matching. The groups differed with regard to disease category with slightly more myelodysplastic syndrome patients ($P = .02$) and a higher CD34-cell dose ($P = .001$) in the PBSC group.

Neutrophil and platelet engraftment were achieved significantly faster after PBSC than BM transplantation (Figure 1A-B). In this entirely pediatric cohort, the incidence of clinically relevant grade II-IV acute GVHD (Figure 1C) did not differ. Most importantly, the incidence of chronic GVHD (PBSCs vs BM: 35% vs 33%, respectively; $P = .9$) and extensive chronic GVHD (Figure 1D) proved low and was virtually identical in the 2 groups. With a median follow-up time of 3 years, overall survival (PBSCs vs BM: 50% ± 5% vs 46% ± 6%, respectively; $P = .63$) and event-free survival (PBSCs vs BM: 45% ± 5% vs 44% ± 6%, respectively; $P = .59$) were comparable (Figure 1E-F). In multivariable analysis, taking into account all parameters with $P < .2$ in univariate analysis, the only significant independent risk factor for treatment failure was advanced disease status at the time of transplantation (relative risk = 2.4, 95% confidence interval, 1.5-3.8; $P = .001$). In contrast, stem cell source (PBSCs vs BM) had no effect (relative risk = 1.1, 95% confidence interval, 0.7-1.6; $P = .8$).

Our registry-based analysis provides evidence that in pediatric recipients of HLA-matched unrelated-donor transplantation with consistent antithymocyte globulin (ATG) use during conditioning, transplantation with PBSCs and BM results in comparable clinical outcomes without detectable differences in the risk of acute or, more importantly, chronic GVHD. Consistent with a recent study underscoring the role of ATG for the prevention of acute and chronic GVHD,[5] the use of ATG in 96% of our transplantation procedures compared with only 27% in the above-mentioned randomized study by Anasetti et al[4] might be one of the key factors responsible for the overall low and comparable incidence of

Teeranaipong P et al. *Journal of the International AIDS Society* 2013, **16**:18723
http://www.jiasociety.org/index.php/jias/article/view/18723 | http://dx.doi.org/10.7448/IAS.16.1.18723

JIAS Journal of the International AIDS Society

Research article

Development of a rapid cell-fusion-based phenotypic HIV-1 tropism assay

Phairote Teeranaipong*[1], Noriaki Hosoya*[2], Ai Kawana-Tachikawa[1], Takeshi Fujii[3], Tomohiko Koibuchi[3], Hitomi Nakamura[2,3], Michiko Koga[1,3], Naoyuki Kondo[4,5], George F Gao[6], Hiroo Hoshino[7], Zene Matsuda[4,5] and Aikichi Iwamoto[§,1,2,3,4]

[§]**Corresponding author:** Aikichi Iwamoto, Division of Infectious Diseases, Advanced Clinical Research Center, Institute of Medical Science, University of Tokyo, 4-6-1 Shirokanedai, Minato-Ku, Tokyo 108-8639, Japan. Tel: +81-3-6409-2202. Fax: +81-3-6409-2008. (aikichi@ra3.so-net.ne.jp, aikichi@ims.u-tokyo.ac.jp)
*These authors contributed equally to this work

Abstract

Introduction: A dual split reporter protein system (DSP), recombining *Renilla* luciferase (RL) and green fluorescent protein (GFP) split into two different constructs (DSP_{1-7} and DSP_{8-11}), was adapted to create a novel rapid phenotypic tropism assay (PTA) for HIV-1 infection (DSP-Pheno).

Methods: DSP_{1-7} was stably expressed in the glioma-derived NP-2 cell lines, which expressed CD4/CXCR4 (N4X4) or CD4/CCR5 (N4R5), respectively. An expression vector with DSP_{8-11} (pRE11) was constructed. The HIV-1 envelope genes were subcloned in pRE11 (pRE11-env) and transfected into 293FT cells. Transfected 293FT cells were incubated with the indicator cell lines independently. In developing the assay, we selected the DSP_{1-7}-positive clones that showed the highest GFP activity after complementation with DSP_{8-11}. These cell lines, designated N4R5-DSP_{1-7}, N4X4-DSP_{1-7} were used for subsequent assays.

Results: The env gene from the reference strains (BaL for R5 virus, NL4-3 for X4 virus, SF2 for dual tropic virus) subcloned in pRE11 and tested, was concordant with the expected co-receptor usage. Assay results were available in two ways (RL or GFP). The assay sensitivity by RL activity was comparable with those of the published phenotypic assays using pseudovirus. The shortest turnaround time was 5 days after obtaining the patient's plasma. All clinical samples gave positive RL signals on R5 indicator cells in the fusion assay. Median RLU value of the low CD4 group was significantly higher on X4 indicator cells and suggested the presence of more dual or X4 tropic viruses in this group of patients. Comparison of representative samples with Geno2Pheno [co-receptor] assay was concordant.

Conclusions: A new cell-fusion-based, high-throughput PTA for HIV-1, which would be suitable for in-house studies, was developed. Equipped with two-way reporter system, RL and GFP, DSP-Pheno is a sensitive test with short turnaround time. Although maintenance of cell lines and laboratory equipment is necessary, it provides a safe assay system without infectious viruses. With further validation against other conventional analyses, DSP-Pheno may prove to be a useful laboratory tool. The assay may be useful especially for the research on non-B subtype HIV-1 whose co-receptor usage has not been studied much.

Keywords: HIV-1; co-receptor; tropism; co-receptor usage; fusion; chemokine receptor.

Received 5 May 2013; **Revised** 10 August 2013; **Accepted** 19 August 2013; **Published** 18 September 2013

Introduction

A new class of drugs to combat HIV-1 infection emerged in 2007 with the marketing approval of maraviroc, a small molecule that binds specifically to the CCR5 co-receptor to block viral attachment and entry [1]. While entry inhibitors are a welcome addition to the antiretroviral arsenal, one problem with this new class of drugs is that treatment is effective only against viruses with the specified co-receptor usage. HIV-1 tropism is defined by the chemokine co-receptors used for viral attachment: R5-tropic viruses use CD4/CCR5, X4-tropic viruses use CD4/CXCR4 and R5X4- or dual-tropic viruses use both CD4/CCR5 and CD4/CXCR4 [2–4]. In clinical treatment with maraviroc, the presence of X4- or dual-tropic viruses is associated with treatment failure [5,6], and a tropism assay is mandatory before treatment initiation.

HIV-1 tropism may be examined genotypically or phenotypically. Genotypic tropism assay (GTA) is based on DNA amplification and sequencing of the third variable (V3) region of the envelope glycoprotein gp120, shown by genetic mapping to be the major determinant of HIV-1 tropism [7–10]. GTA has advantages of platform portability, low cost and rapid turnaround time [11]; however, the interpretation of the sequences is complicated because of the high variability [12]. The assay used in association with maraviroc treatment is the phenotypic tropism assay (PTA) Trofile™ (Monogram Biosciences Inc., CA, USA), a CD4 cell culture assay using replication-defective pseudoviruses [13]. Although Trofile™ is

considered the gold standard, a simpler and effective PTA would be useful.

Here, we describe a novel, cell-fusion-based PTA that uses a dual split reporter protein system (DSP) [14,15] to measure HIV-1 tropism by both Renilla luciferase (RL) activity and green fluorescent protein (GFP) activity. We validated the DSP-Pheno assay using HIV-1 reference strains and applied the assay to test clinical samples from patients with HIV-1 infection.

Methods

Approval of the study and recombinant DNA experiments

Plasma samples from HIV-1-positive patients attending the hospital affiliated with the Institute of Medical Science, the University of Tokyo (IMSUT) were collected and kept frozen until use. Patients provided written informed consent, and the study was approved by the Institutional Review Board of the University of Tokyo (approval number 20-31). Recombinant DNA experiments used in this work were approved by the Institutional Review Board (approval number 08-30), and by the review board in the Ministry of Education, Culture, Sports, Science and Technology (MEXT; approval number 23-1927).

Cell lines

Cell lines N4, N4X4 and N4R5 are derived from the human glioma NP-2 cell line and stably express CD4, CXCR4 and CCR5, respectively [16,17]. NP-2-derived cell lines were grown in M10+ medium (modified Eagle's medium (MEM; Sigma, St. Louis, MO, USA) supplemented with 10% heat-inactivated foetal bovine serum (FBS), 100 units/ml of penicillin and 0.1 mg/ml of streptomycin). 293FT cells (Invitrogen, Carlsbad, CA, USA) were grown in D10+ medium (Dulbecco's modified Eagle's medium (DMEM, Sigma) supplemented with 10% FBS, 100 units/ml of penicillin and 0.1 mg/ml of streptomycin). All cell cultures were maintained at 37°C in a humidified 5% CO_2 incubator.

Reference viral envelopes

The plasmids encoding reference HIV-1 envelopes with well-characterized co-receptor usage were obtained from NIH AIDS Research & Reference Reagent Program (NIH ARRRP: Germantown, MD, USA). NL4-3 and LAI represented X-4 tropic viruses; BaL represented R5-tropic viruses; and SF2 represented dual (R5X4)-tropic viruses. The co-receptor usage of these laboratory strains has been published [13,18–22].

Construction of DSP expression plasmids

The DSP system utilizes a pair of chimeric reporter proteins, DSP_{1-7} and DSP_{8-11}, each of which is a fusion of split green fluorescent protein (spGFP) and split Renilla luciferase (spRL) [15]. DSP_{1-7} fuses the N-terminal region of RL (amino acids 1–229) to the N-terminal region of GFP (amino acids 1–157), with a linker sequence separating the two regions. DSP_{8-11} has the complementary structure, with the C-terminal region of GFP (amino acids 158–231), fused to the C-terminal region of RL (amino acids 230–311), also separated by a linker sequence. When both reporter proteins are present in the same cell, they each recover full activity.

To generate pLenti-DSP_{1-7} plasmid, we first amplified an attB-flanked DSP_{1-7} fragment (1251 bp) using pDSP $_{1-7}$ as a template and attB-flanked primers [attB1-DSP1-1F (56-mer, 5′-GGGGACAAGTTTGTACAAAAAAGCAGGCTGGGCTAGCCACCA TGGCTTCCAAGGTG -3′) and attB2-DSP1-1R (51-mer, 5′-GG GGACCACTTTGTACAAGAAAGCTGGGTGCTCTAGATCACTTGT CGGCGG-3′)]. Sequential amplicons were transferred to pDONR-221 and pLenti6.3/V5-DEST (Invitrogen) using the ViraPower™ HiPerform™ Lentiviral Gateway® Expression System (Invitrogen) according to the manufacturer's protocol. Constructs were verified by sequencing.

An expression vector, pRE11 (Figure 1), was constructed for the co-expression of DSP_{8-11} and HIV-1 *env* by multiple rounds of PCR and subcloning. Source plasmids were pIRES2-AcGFP1 (Clontech), pmOrange (Clontech), $pDSP_{8-11}$ [15] and pmirGLO (Promega). pRE11 incorporated multiple cloning sites under the PGK promoter for the insertion of HIV-1 *env* (Shown as 5′-XbaI-XhoI-3′ in Figure 1b). Necessary restriction enzyme cleavage sites used for construction, including multiple cloning sites (XbaI-MluI-SwaI-AgeI-XhoI), were created using synthetic oligonucleotides and PCR. A CMV promoter drives $pDSP_{8-11}$ directly. The same CMV promoter expresses mOrange with a nuclear localization signal that serves as a marker for successful transfection via internal ribosomal entry site (IRES). All PCR fragments were confirmed by sequencing.

NP-2-derived fusion indicator cell lines

We used the ViraPower Packaging Mix with Lipofectamine 2000 (Invitrogen) to transfect 293FT cells with pLenti-DSP_{1-7} and create pseudoviruses containing the DSP_{1-7} expression cassette (Lenti-DSP_{1-7}). We next infected cell lines NP-2/CD4 (N4), CD4/CXCR4 (N4X4) and CD4/CCR5 (N4R5) with pseudoviruses containing LentiDSP_{1-7} for 2 hours. Cells were distributed in 96-well tissue culture plates at a density of 75 cells/plate (0.8 cell/well) and grown in the presence of 4 μg/ml blasticidin. Approximately 50 candidate clones from each cell line were randomly selected and tested for FITC intensity using FACS Calibur (BD Biosciences, Franklin Lakes, NJ, USA) 48 hours after transfection of $pDSP_{8-11}$. FACS data were analyzed by Flow Jo version 8.7.1 (Tree Star Inc., OR, USA). Clones with the highest median FITC intensity were expanded in M10+ supplemented with 4 μg/ml of blasticidin (M10 + 4) for further assays.

Generation of pRE11-env strains

Full-length HIV-1 *env* was prepared by PCR amplification from clinical plasma samples as described [23]. Viral RNA was extracted from 140 μl of patient's plasma by QIAamp Viral RNA Mini kit according to the manufacturer's recommendation (QIAGEN, Hilden, Germany). One-step RT-PCR using SuperScript III and High Fidelity Platinum® Taq DNA polymerase (Invitrogen) was carried out in five separate 15-μl reactions to minimize the bias created by PCR. The reaction mixture contained 2 μl of RNA template, 7.5 μl of 2 × reaction buffer, 0.3 μl of 5 mM $MgSO_4$, 0.3 μl of each 10 μM of forward primer (Env-1F, 25-mer, 5′-TAGAGCCCTG GAAGCATCCAGGAAG-3′) and reverse primer (Env-3Rmix, equimolar mixture of 30-mer, 5′ -TGCTGTATTGCTACTTGTGATTGCTCCATA-3′ and 30-mer, 5′ -TGCTGTATTGCTA CTTGTGATTGCTCCATG-3′), 0.6 μl of

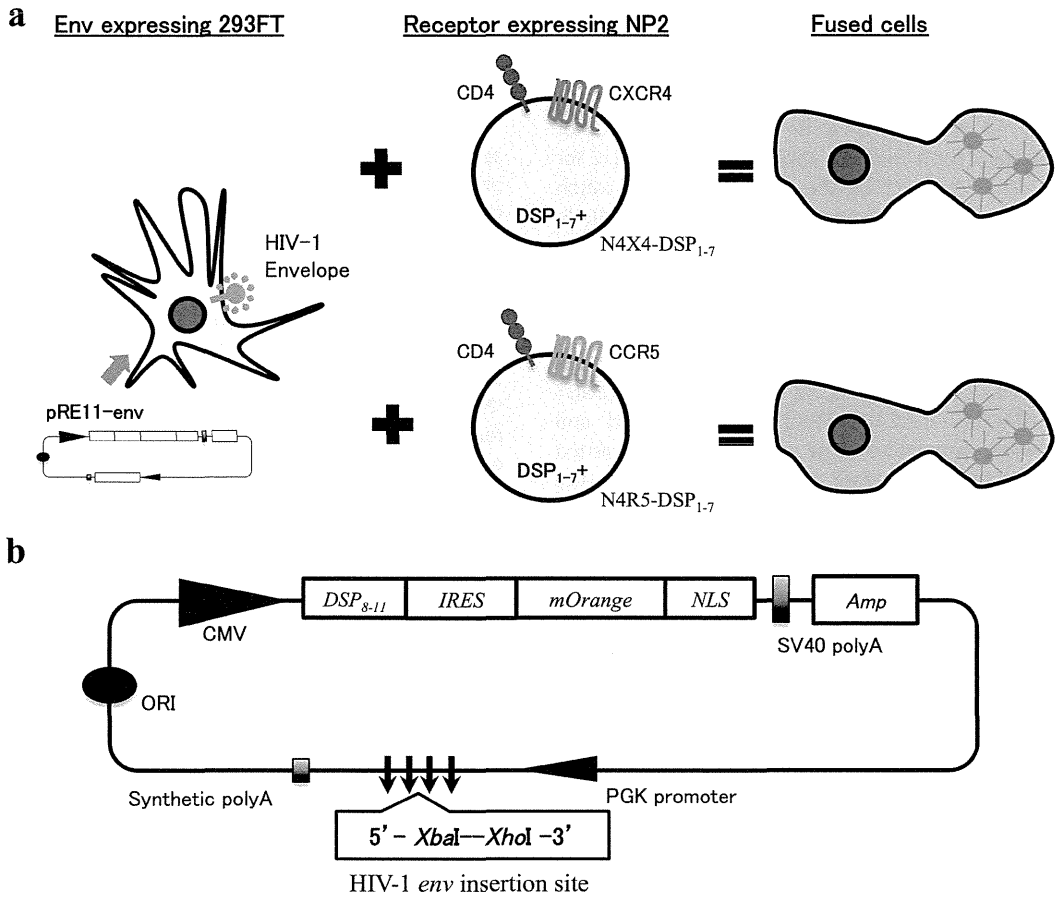

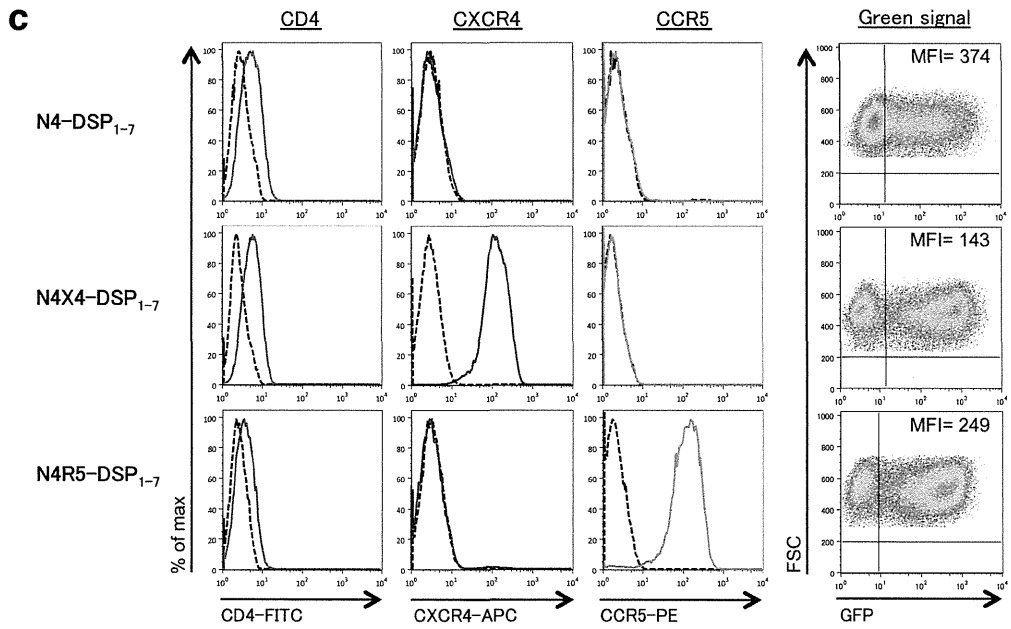

Figure 1. A cell-fusion-based phenotypic tropism assay for HIV-1: DSP-Pheno. (a) Schematic representation of DSP-Pheno assay system. (b) Schematic representation of pRE11, an expression vector for HIV-1 env and DSP_{8-11}. pRE11 encodes also mOrange with a nuclear localization signal as an indicator of transfection. (c) NP-2-derived clones stably expressing DSP_{1-7} (N4-DSP_{1-7}, N4X4-DSP_{1-7} and N4R5-DSP_{1-7}) were selected by the high GFP expression after direct transfection of $pDSP_{8-11}$. The expression of CD4/co-receptors was reconfirmed by appropriate monoclonal antibodies and FACS analysis.

SuperScript III and High Fidelity Platinum® Taq DNA polymerase, 0.25 μl of RNAse OUT and 3.75 μl of nuclease-free water with the final volume of 15 μl/reaction. The one-step RT-PCR condition was 55°C for 30 minutes, 94°C for 2 minutes followed by 30 cycles of 94°C for 20 seconds, 55°C for 30 seconds, 68°C for 4 minutes, then extension at 68°C for 5 minutes. The fragment by the first-round amplification extended from NL4-3 reference position of 5853–8936. Products from five independent reactions were combined. Four microliters of the mixed first-round PCR products were used as the template for each of five independent second-round PCR reactions employing EnvB-2F-Xba (41-mer, 5′-TAGCTCTAGAACGCGTCTTAGGCATCTCCTATGGCAG GAAG-3′) and EnvB-4R-Xho (41-mer, 5′ -TAGCCTCGAGACCGGT TACTTT TTGACCACTTGCCACCCAT-3′) as the forward and reverse primers, respectively. The second PCR was carried out according to the standard 50-μl PCR protocol of the Platinum® PCR SuperMix High Fidelity as described above. The fragments amplified by the second PCR extended from NL4-3 reference position of 5957–8817. After digestion with Xba I and Xho I, about 3-kb PCR products were purified by 1.2% agarose gel and QIAquick gel extraction kit (Qiagen). The purified products were inserted into pRE11 at XbaI and XhoI sites, resulting in HIV-1*env* expression plasmid (pRE11-envbulk) from each patient. pRE11-envbulk, representing a quasispecies of *env* population from each patient, was prepared by transfecting into *E. coli* JM109. For bulk analysis, transfected JM109 was expanded to 25 ml, followed by QIAGEN Plasmid Midi Kit (Qiagen) for DNA extraction.

Cell-fusion assay

On the day before transfection, 500 μl aliquots of 293FT cells in DMEM supplemented with 10% FBS (D10) were seeded in 24-well tissue culture plates at a density of 2.8×10^5 cells/well and incubated overnight to 70–80% confluency. The cells were then transfected with pRE11-envstrain or pRE11-envbulk according to the manufacturer's protocol (Roche). On the same day, 100 μl aliquots of N4-DSP_{1-7}, N4X4-DSP_{1-7} and N4R5-DSP_{1-7} cells in MEM supplemented with 10% FBS (M10) were seeded in a 96-well tissue culture, optical bottom plate (NUNC, Thermo Fisher Scientific Inc., NY, USA) at a density of 1×10^4 cells/well and incubated at 37°C. Forty-eight hours after transfection, the medium of transfected 293FT cells was removed by aspiration and replaced with 1 ml of PBS (Sigma) at RT. Transfected 293FT cells were resuspended by gentle pipetting.

To start the cell-fusion assay, 150 μl/well of transfected cells were overlaid onto N4-DSP_{1-7}, N4X4-DSP_{1-7} and N4R5-DSP_{1-7} cells. The cells were incubated for fusion at 37°C in a humidified 5% CO_2 incubator for 6 hours, and then analyzed by automatic image capture using an In Cell Analyzer 1000 (GE Healthcare). Four fields/well of image were captured through red, green and bright field channels, and fused cells were identified by the presence of two or more red nuclei surrounded by a green area (cytoplasm). Immediately after image capturing, EnduRen™ Live Cell Substrate (Promega) was added to each well, and luciferase activity was measured three times using a Glomax 96 microplate luminometer (Promega), according to the manufacturer's instructions. The mean luciferase activity, recorded as relative light unit (RLU), was the average of three measurements per well. The experiments were conducted in triplicates and repeated independently at least three times.

To test the co-receptor specificity, 2 μM/well of the appropriate inhibitor was added to the cells 90 minutes prior to the cell-fusion assay (CXCR4 inhibitor AMD3100 (Sigma) to N4X4-DSP_{1-7} cells and CCR5 inhibitor maraviroc (Sigma) to N4R5-DSP_{1-7} cells).

Genotyping

pRE11-envbulk were sequenced in both the 5′ and 3′ directions using population-based sequencing on the ABI 3130xl genetic analyzer (Applied Biosystems, Foster City, CA, USA) using BigDye Terminator V3.1 (Applied Biosystems) with forward primer E110 (5′ -CTGTTAAATGGCAGTCTAGCAGAA-3′), and reverse primer Er115 (5′ -AGAAAAATTCCCCTCCACAATT AA-3′). The V3 nucleotide sequences were submitted to the Geno2Pheno (co-receptor) algorithm (http://coreceptor.bioinf.mpi-inf.mpg.de) setting the false positive rate (FPR) at 10%.

Results

Construction of DSP_{1-7} and DSP_{8-11} expression vectors

We inserted DSP_{1-7} or DSP_{8-11} sequences into blasticidin-resistant lentivirus vectors and then infected NP-2/CD4 (N4), NP-2/CD4/CXCR4 (N4X4) and NP-2/CD4/CCR5 (N4R5) cells with the recovered pseudoviruses, selecting for blasticidin-resistant clones. We screened 49, 51 and 43 lentivirus-infected and blasticidin-resistant clones from N4, N4X4 and N4X5, respectively, for high levels of DSP_{1-7} or DSP_{8-11} expression following super-transfection with the complementary plasmid (pDSP_{8-11} or pDSP_{1-7}, respectively). From each of the cell lines, we selected the blasticidin-resistant and DSP_{1-7}-positive clone that showed the highest GFP activity after complementation with DSP_{8-11}. These cell lines, designated N4-DSP_{1-7}, N4X4-DSP_{1-7} and N4R5-DSP_{1-7}, were re-evaluated for their expression of CD4, CXCR4 and CCR5 on the cell surface (Figure 1c).

Using this approach, we obtained N4- and N4R5-cells expressing high levels of DSP_{8-11}, but were unable to obtain a stable N4X4 cell line expressing DSP_{8-11} (data not shown). To circumvent this problem, we decided to generate 293FT cells transiently expressing both DSP_{8-11} and the HIV-1 *env* protein and develop a cell-fusion assay system using those cells together with the NP-2-derived cells stably expressing DSP_{1-7} (Figure 1a). Thus, we constructed the expression vector pRE11, containing the DSP_{8-11} expression cassette and cloning sites for insertion of HIV-1 *env* sequences under the control of the PGK promoter (Figure 1b).

Validation of the cell-fusion assay using the *env* gene from laboratory HIV-1 strains

We validated the DSP assay system (DSP-pheno) using pRE11 constructs engineered to contain *env* sequences from reference strains with known co-receptor usage. The *env* reference constructs, which also contained the DSP_{8-11} expression cassette, were the following: pRE11-HXB2, pRE11-LAI, and pRE11-NL4-3 (X4 strains); pRE11-BaL (R5 strain); and pRE11-SF2 (dual strain). The cell-fusion assays were performed with N4X4-DSP_{1-7} or N4R5-DSP_{1-7} cells in

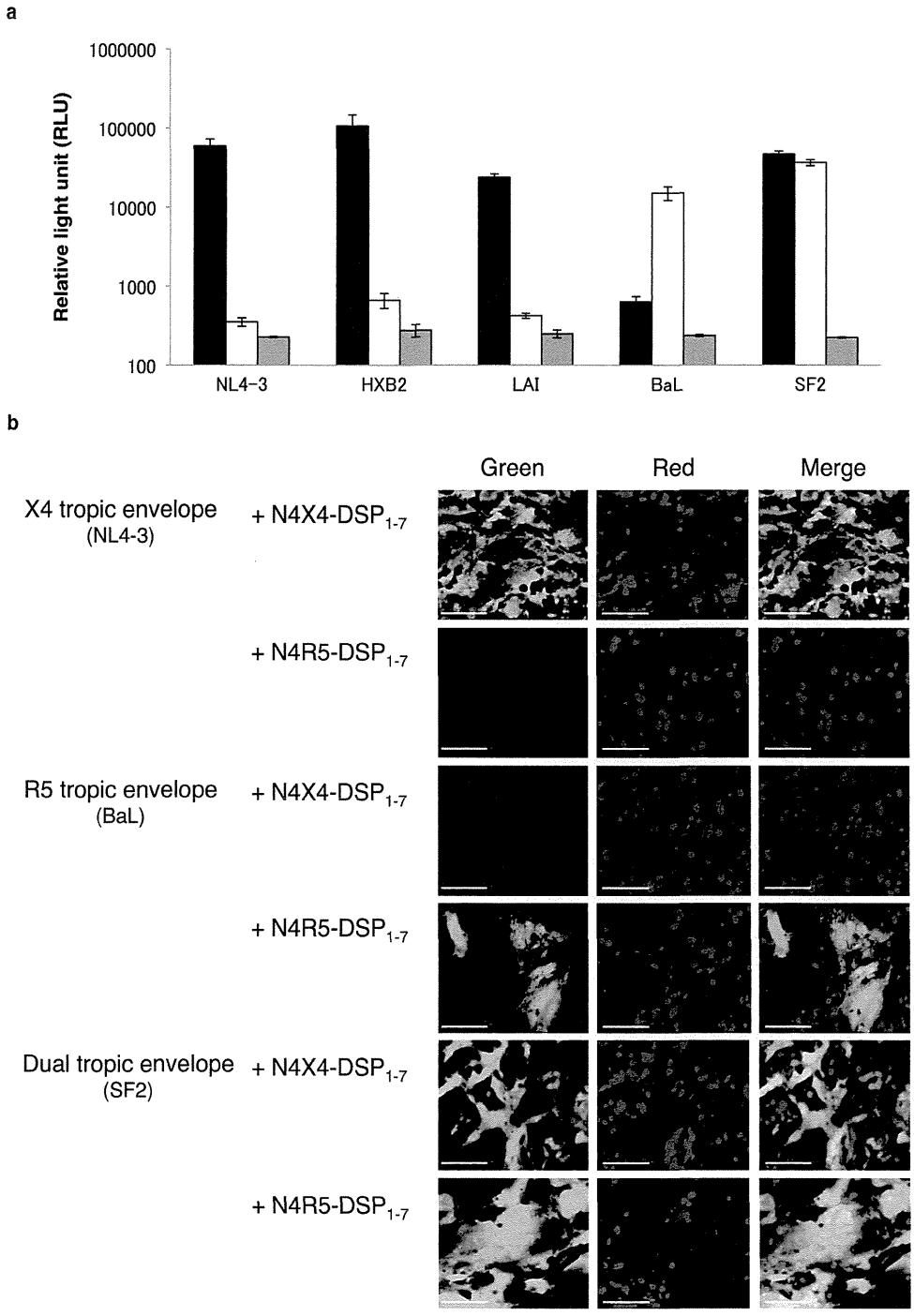

Figure 2. Validation of the cell-fusion assay using env genes from HIV-1 reference strains. (a) RL activities after cell fusion were measured using NL4-3, HXB2 and LAI as X4 reference strains while BaL or SF2 as R5 or R5X4 strains, respectively. Black columns: RL activities on N4X4-DSP$_{1-7}$. White columns: activities on N4R5-DSP$_{1-7}$. Grey columns: activities on N4-DSP$_{1-7}$. Small bars at the top of each column indicate the mean RLU $\pm$ SD from three independent experiments. (b) Successful cell fusion is indicated by the green fluorescence in the cytoplasm. Red spots were mOrange activity in the nuclei showing successful transfection. Merged images showed multinuclear cells with multiple yellow/orange nuclei surrounded by green cytoplasm.

combination with 293FT cells transiently expressing one of the pRE11-env constructs. In all the assays, both RL and GFP activities were restored only when cells expressing the appropriate *env* and co-receptor combinations were co-cultured (Figure 2a and b). Co-culture of N4X4-DSP$_{1-7}$ or N4R5-DSP$_{1-7}$ in combination with the 293FT cells transiently expressing the pRE11-env constructs of discordant tropism served as a negative control for expression of RL activities

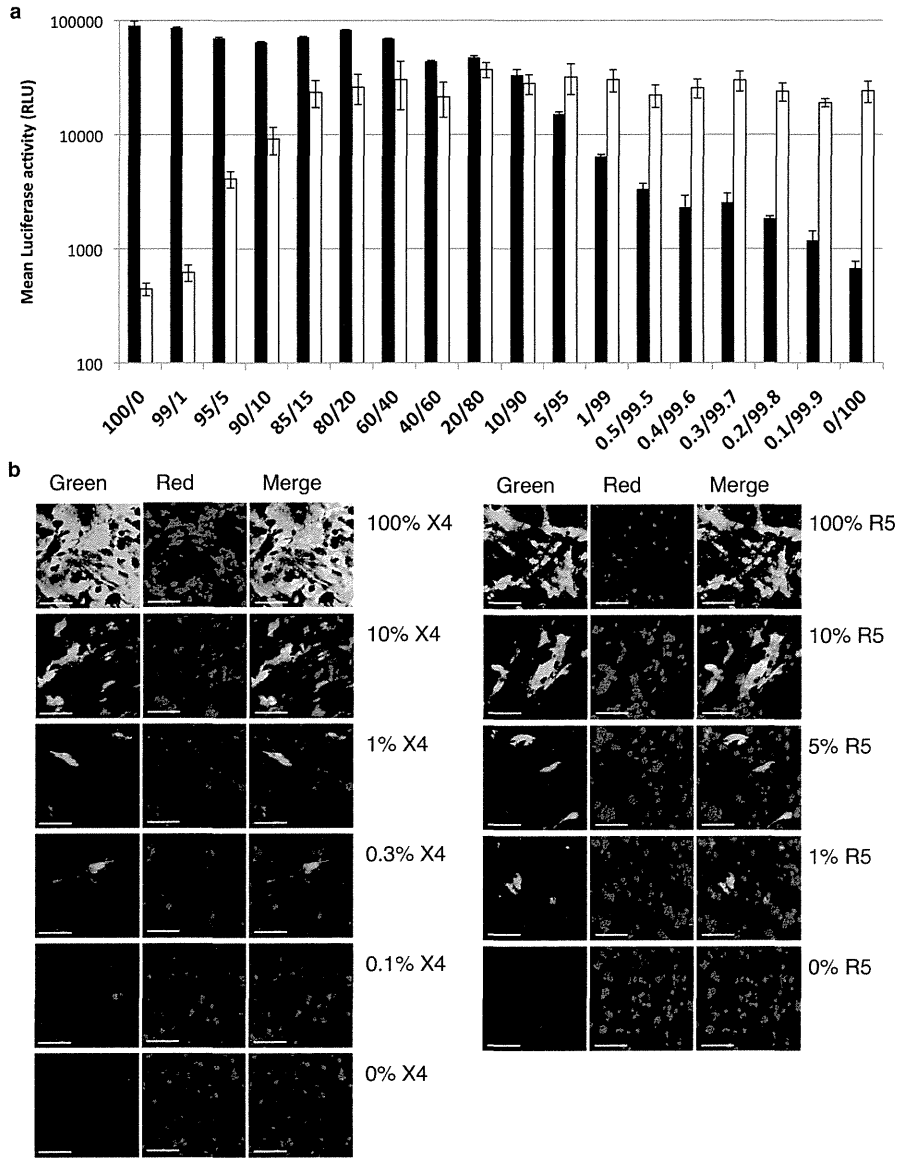

Figure 3. Assay sensitivities for minor populations. pRE11-NL4-3 (X4) and pRE11-BaL (R5) were mixed at indicated ratios. The total plasmid concentration in the mixture was adjusted to 100 ng/μl. The mixture was transfected to 293FT cells and fused to the indicator cells. (a) RL activities. Black columns show the RL activities on X4 indicator (N4X4-DSP$_{1-7}$), while white columns on R5-indicator (N4R5-DSP$_{1-7}$). Small bars at the top of each column indicate the mean RLU ± SD from three independent experiments. (b) GFP activities. Left panel shows activities of the mixture with indicated ratio on X4 indicator (N4X4-DSP$_{1-7}$), while right panel on R5-indicator (N4R5-DSP$_{1-7}$).

(Figure 2a) and GFP signals (Figure 2b). The absence of RL activities on N4-DSP$_{1-7}$ confirmed the importance of co-receptors for the fusion.

Assay detection thresholds and sensitivity for minor populations

To evaluate assay sensitivity in identifying minor variants within a single sample, we mixed pRE11-NL4-3 (X4) and pRE-BaL (R5) in varying ratios and measured RL activities and GFP signals (Figure 3a and b). Both methods of detection identified X4 viruses more readily than R5 viruses. Based on luciferase activity, the presence of approximately 0.3% X4 viruses gave values significantly higher than background (0% X4), while R5 viruses had to comprise approximately 5% of the mixture for the signal to be detectable over background (Figure 3a). Similarly, based on GFP signals, X4 viruses comprising as little as 0.1% of the mixture could be detected, while detection of R5 viruses had a minimum threshold of approximately 1% (Figure 3b).

Validation of the chemokine receptor specificity using the CXCR4 inhibitor AMD3100 and CCR5 inhibitor maraviroc

293FT cells expressing *env* from reference strains NL4-3 (X4) or BaL (R5) were co-cultured with N4X4-DSP$_{1-7}$ or N4R5-DSP$_{1-7}$ cells in the absence or presence of AMD3100 or maraviroc (Figure 4a and b). In the absence of inhibitors, RL activities of

the matched co-culture were high (Figure 4a). In the presence of AMD3100, the RL activity of the co-culture of 293FT cells expressing NL4-3-derived *env* with N4X4-DSP_{1-7} cells was reduced by 83%. The RL activity of the co-culture of 293FT cells expressing BaL-derived *env* with N4X4-DSP_{1-7} cells was low in the absence of AMD3100 and was not affected significantly by its presence. The RL activity of the co-culture of 293FT cells expressing BaL-derived *env* with N4R5- DSP_{1-7} was reduced by 81% in the presence of maraviroc. The RL activity of the co-culture of 293FT cells expressing NL4-3-derived *env* with N4R5- DSP_{1-7} was low regardless of the presence or absence of maraviroc. The results indicated that DSP-Pheno could be used as an assay for entry inhibitors.

Cell-fusion assay of clinical samples

To evaluate assay performance using clinical samples, we selected plasma samples from 101 treatment-naïve, HIV-1-positive patients, whose infection with clade B viruses had been confirmed (data not shown). The patient population was classified into two groups based on CD4 T cell count. The low CD4 group consisted of 57 patients with CD4 T cell counts <350 cells/μl; median 228 (range 2–350) cells/μl, and median viral load was 4.77 (range 2.97–6.62) log 10 copies/ml (Figure 5a and b). The high CD4 group consisted of 44 patients with CD4 cell counts >350 cells/μl; median 442 (range 351–843) cells/μl, and median viral load was 4.04 (range 1.60–5.41) log 10 copies/ml. The viral load differences

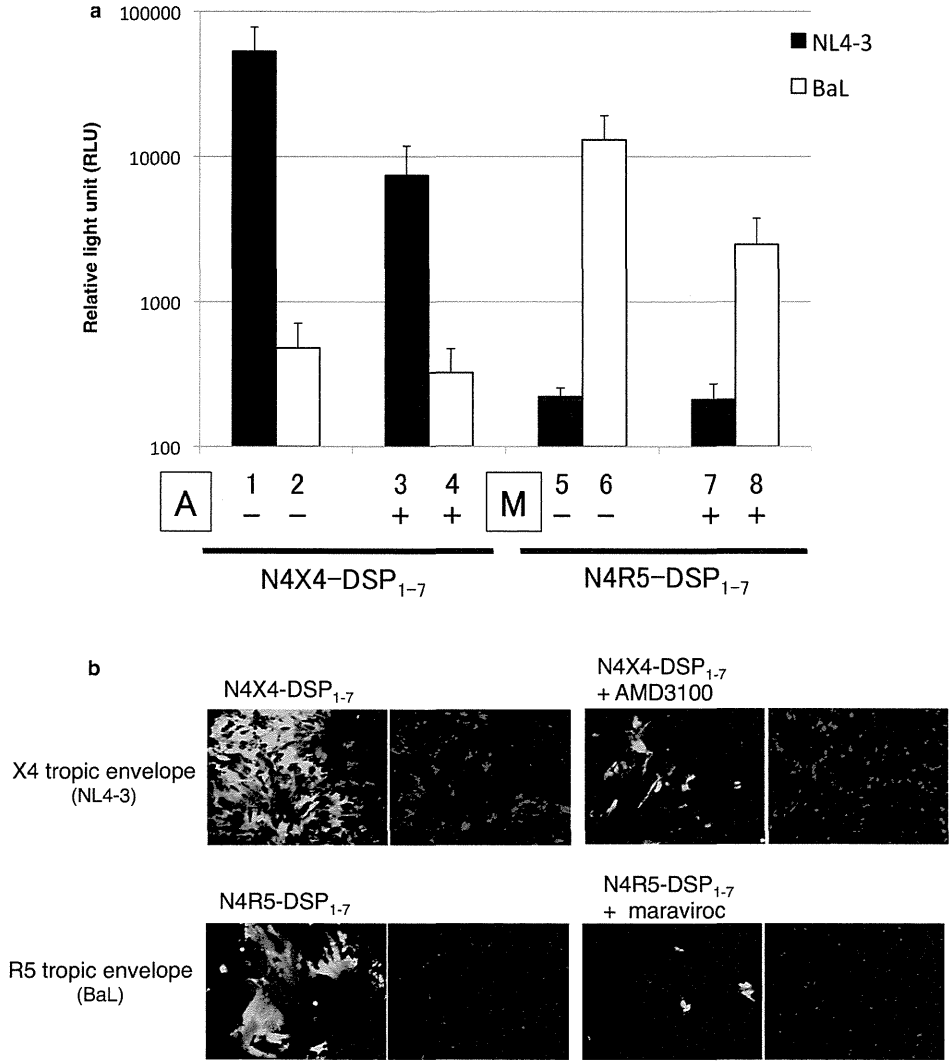

Figure 4. Inhibition of cell fusions by entry inhibitors. Two μM/well of CXCR4 inhibitor AMD3100 or CCR5 inhibitor maraviroc were added into N4X4-DSP_{1-7} and N4R5-DSP_{1-7} cells 90 minutes prior to cell-fusion assay using env derived from reference strains.(a) RL activities. Columns show the mean RLU ± SD from 5 independent experiments. Black columns, RL activities of env derived from X4 reference strain (NL4-3); white columns, RL activities of env derived from R5 reference strain (BaL). Results from X4-indicator (N4X4-DSP_{1-7}) (lanes 1–4) and R5-indicator (N4R5-DSP_{1-7}) (lanes 5–8). A, AMD3100; M, maraviroc. Presence or absence of inhibitor indicated by + or –, respectively. (b) GFP activities. Green fluorescence in the left panel of each pair shows successful cell fusions; red spots in the right panels show the successful transfection. Reference strains, indicator cells and inhibitors used are shown in the figure.

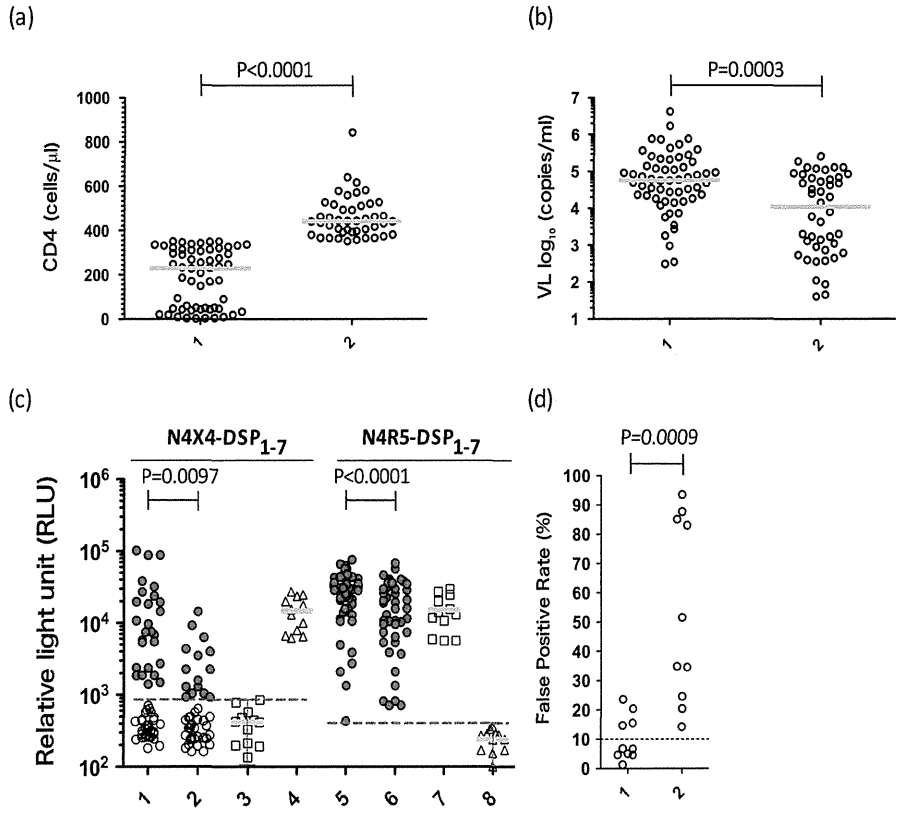

Figure 5. DSP-Pheno and Geno2Pheno on clinical samples. Patients were assigned to one of the two groups based on CD4+ T cell counts. Horizontal green bars indicate the median value. (a) CD4 counts of the patients. Lane 1, Fifty-seven patients with CD4 <350 cells/μl, median =228 (range 2–350) cells/μl. Lane 2, Forty-four patients with CD4 >350 cells/μl, median 442 (range 351–843) cells/μl. (b) Viral load of each group. Lane 1, CD4 <350 group, median viral load =4.77 (range 2.97–6.62) log10 copies/ml. Lane 2, CD4 <350 group, median viral load =4.04 (range 1.60–5.41) log 10 copies/ml. (c) Mean luciferase activities of the patients' plasma samples. Lanes 1 and 5, CD4 <350 group; lanes 2 and 6, CD4 >350 group; lanes 3 and 7, R5 controls (BaL); lanes 4 and 8, X4 controls (NL4-3). Dashed red lines are the cut-off value, that is, the mean value+2SD based on 3 three determinations in 12 independent experiments for each combination of negative control and indicator cell. (d) Geno2Pheno [co-receptor] analysis of representative samples. Lane 1, 10 samples from dual/X4 [N4X4-DSP$_{1-7}$ (+), N4R5-DSP$_{1-7}$ (+)] group by DSP-Pheno; Lane 2, 10 samples from R5 [N4X4-DSP$_{1-7}$ (−), N4R5-DSP$_{1-7}$ (+)] group by DSP-Pheno. For dual/X4 and R5 group, five patients each from CD4 < 350 and CD4 >350 groups were chosen. Dashed line indicates the cut-off value as 10% of FPR.

between the two groups were statistically significant by the Mann–Whitney *U* test ($p < 0.001$). Aliquots of viral envelope DNA from each plasma sample were used to construct pRE11-envbulk for transfection into 293FT cells. The plasma viral load necessary for the assay was roughly 3.00 log 10 copies/ml for subtype B viruses, although we could amplify the env gene in a patient with 1.60 log 10 copies/ml.

We used the laboratory strain, BaL as the R5 control and NL4-3 as the X4 control to define the cut-off values. We examined BaL on N4X4-DSP$_{1-7}$ cells and NL4-3 on N4R5-DSP$_{1-7}$ cells. We defined the cut-off value tentatively as the mean value+2SD based on 3 determinations in 12 independent experiments for each combination of negative control and indicator cell (red dashed line in Figure 5c). As expected, both combinations showed stably low RL activities, with cut-off values of 876 for N4X4-DSP$_{1-7}$ cells and 397 RLU for N4R5-DSP$_{1-7}$ cells.

Samples from all patients gave positive RL signals on R5 indicator cells (N4R5-DSP$_{1-7}$) in the fusion assay, which suggested that the bulk of virus in each patient was able to use CCR5 as the co-receptor (Figure 5c, lanes 5 and 6). Median RLU value of the low CD4 group was significantly higher than that of the high CD4 group on R5 indicator cells ($p < 0.0001$). Median RLU value of the low CD4 group was also higher significantly on X4 indicator cells ($p = 0.0097$) and 26/57 (46%) of low CD4 cases versus 15/44 (34%) of high CD4 cases gave positive RL signals (Figure 5c, lanes 1 and 2). Higher fusion activities on both indicator cells are compatible with higher viral loads in patients with lower CD4 T cell counts and may suggest more dual or X4 tropic (dual/X4) viruses in this group of patients.

To compare the result with conventional GTA, we selected 10 samples each from dual/X4 [N4X4-DSP$_{1-7}$ (+), N4R5-DSP$_{1-7}$ (+)] and R5 [N4X4-DSP$_{1-7}$ (−), N4R5-DSP$_{1-7}$ (+)] cases. Env V3 nucleotide sequences from pRE11-envbulk plasmids were subjected to the Geno2Pheno [co-receptor]. R5-representative samples showed significantly higher FPR than dual/X4-representative samples ($p = 0.0009$) (Figure 5d). DSP-Pheno and Geno2Pheno gave concordant results in 10/10 R5 and 6/10 dual/X4 samples (Figure 5d).

Although there were four samples with discordant result in dual/X4 samples, FPR of these samples were low (range: 14.7–23.6%).

Discussion

We developed a quick, safe and sensitive HIV-1 PTA utilizing double split proteins (DSP-Pheno) and validated the specificity of the assay using laboratory strains with known co-receptor usage. We recognize several limitations of this preliminary study, but the results nevertheless are promising. We assayed bulk envelope genes amplified from plasma from HIV-1-infected patients, rather than cloned envelope genes, and our sample only included subtype B HIV-1. Future studies are necessary to demonstrate the usefulness of the DSP-Pheno.

One caveat of the DSP-Pheno assay is that it is a cell-fusion system, and cell–cell fusion may differ in significant details from virus–cell fusion. For example, recent studies have shown that HIV-1 virions carry fewer surface glycoproteins than previously assumed [24]. The DSP-Pheno assay uses neuroglyoma cell-derived NP-2 cell lines with overexpressed CD4 and co-receptors. Although these NP-2-derived cell lines have been characterized extensively [16,17], some unknown cell surface molecules may be involved in the fusion process. The DSP-Pheno assay is a gag-free system and requires only the assembly of reporter proteins pre-formed in the fusion partner, but infection by a retrovirus requires that the entire gag particle pass through the fusion pore. Careful comparison between DSP-Pheno and in-house pseudoviral assay or GTA using clonal clinical isolates is under way.

GFP portion is necessary as a module of DSP to compensate weak self-association of split RL [15]. Although RL would be more suitable for quantitative assay, GFP may prove single clear positive fusion in the sample with very low RL readout. This feature of DSP-Pheno incorporating two different assays may be useful for certain scientific purposes.

Although several issues remain to be clarified, DSP-Pheno has multiple advantages over the conventional pseudoviral PTA: (i) the turnaround time for DSP-Pheno is short, with results available in as few as 5 days, starting from patients' plasma; (ii) DSP-Pheno is a virus-free assay that does not require a special biosafety facility, making it particularly appealing for in-house use; and (iii) the RL assay in DSP-Pheno has high sensitivity and specificity and compares favourably with the best pseudoviral PTA published in the detection of minor X4 populations using laboratory strains. Trofile™ (Monogram Biosciences Inc., CA, USA) is currently the only commercially available PTA approved for clinical use, and the latest version, "Enhanced Trofile™," detects X4 minor populations present in concentrations as low as 0.3% [25]. A pseudoviral PTA described by Soda and colleagues had 1% detection threshold for X4 viruses [16]. Although the RL assay in DSP-Pheno could detect X4 laboratory strains present in concentrations as low as 0.3%, further studies are needed to apply the assay for the clinical use. DSP-Pheno may also be useful for the comparison of with GTA to improve the algorithm for the co-receptor usage of non-B subtypes.

Conclusions

We described a new cell-fusion-based, high-throughput PTA for HIV-1, which would be suitable for in-house studies. Equipped with a two-way reporter system, RL and GFP, DSP-Pheno is sensitive and offers a short turnaround time. Although maintenance of cell lines and laboratory equipment for the assay is necessary, it provides a safe assay system without infectious viruses. With further validation against other conventional analysis, DSP-Pheno may prove to be a useful laboratory tool. The assay may be useful especially for the research on non-B subtype HIV-1 whose co-receptor usage has not been studied much.

Authors' affiliations

[1]Division of Infectious Diseases, Advanced Clinical Research Center, Institute of Medical Science, University of Tokyo, Tokyo, Japan; [2]Department of Infectious Disease Control, International Research Center for Infectious Diseases, Institute of Medical Science, University of Tokyo, Tokyo, Japan; [3]Department of Infectious Diseases and Applied Immunology, Affiliated Hospital to Institute of Medical Science, University of Tokyo, Tokyo, Japan; [4]Research Center for Asian Infectious Diseases, Institute of Medical Science, University of Tokyo, Tokyo, Japan; [5]Japan–China Joint Laboratory of Structural Virology and Immunology, Institute of Biophysics, Chinese Academy of Sciences, Beijing, China; [6]CAS Key Laboratory of Pathogenic Microbiology and Immunology, Institute of Microbiology, Chinese Academy of Sciences, Beijing, China; [7]Gunma University Graduate School of Medicine, Gunma University, Gunma, Japan

Current affiliation

Phairote Teeranaipong, Department of Parasitology, Faculty of Medicine, Chulalongkorn University, Bangkok, Thailand.
Takeshi Fujii, Tokyo Medical University, Hachioji Medical Center, Tokyo, Japan.

Competing interests

AI has received grant support from Toyama Chemical Co. Ltd., Astellas, ViiV Healthcare KK, MSD KK, Baxter through the University of Tokyo. AI has received speaker's honoraria/payment for the article from Eiken Chemical Co. Ltd., Astellas, Toyama Chemical Co. Ltd, Torii Pharmaceutical Co. Ltd., Takeda Pharmaceutical Co. Ltd. and MSD.
For the remaining authors, there are no competing interests.

Authors' contributions

PT, NH and AI planned the experimental design. PT and NH did the experiments. NK, ZM and HH provided the materials. ZM, HH, AK-T and GFG and joined the discussion. TF, TK, HN, MK and AI were responsible for the patient care and provided clinical information. PT, NH and AI wrote the article. PT and NH contributed equally to the work.

Acknowledgements

This work was supported in part by a contract research fund from the Ministry of Education, Culture, Sports, Science and Technology (MEXT) for Program of Japan Initiative for Global Research Network on Infectious Diseases (10005010) (AI); Global COE Program (Center of Education and Research for Advanced Genome-Based Medicine – For personalized medicine and the control of worldwide infectious diseases) of MEXT (F06) (AI); JSPS KAKENHI (25293226) (AKT); JSPS KAKENHI (24790437) (NH); Grants for AIDS research from the Ministry of Health, Labor, and Welfare of Japan (H24-AIDS-IPPAN-008) (AKT); Grants for AIDS research from the Ministry of Health, Labor, and Welfare of Japan (H25-AIDS-IPPAN-006) (NH); Research on international cooperation in medical science, Research on global health issues, Health and Labour Science Research Grants, the Ministry of Health, Labor, and Welfare of Japan (H25-KOKUI-SITEI-001) (AI).
The authors thank Ms. Barbara Rutledge for discussion and editing English.

References

1. Dorr P, Westby M, Dobbs S, Griffin P, Irvine B, Macartney M, et al. Maraviroc (UK-427,857), a potent, orally bioavailable, and selective small-molecule inhibitor of chemokine receptor CCR5 with broad-spectrum anti-human immunodeficiency virus type 1 activity. Antimicrob Agents Chemother. 2005;49(11):4721–32.